Dynamic BOTDA measurements based on Brillouin phase-shift and RF demodulation

Javier Urricelqui, Ander Zornoza, Mikel Sagues, and Alayn Loayssa*

Departamento de Ingeniería Eléctrica y Electrónica, Universidad Pública de Navarra Campus Arrosadia s/n, 31006 Pamplona, Spain

alayn.loayssa@unavarra.es

Abstract: We demonstrate a novel dynamic BOTDA sensor based, for the first time to our knowledge, on the use of the Brillouin phase-shift in addition to the conventional Brillouin gain. This provides the advantage of measurements that are largely immune to variations in fiber attenuation or changes in pump pulse power. Furthermore, the optical detection deployed leads to an enhanced precision or measurement time and to the broadening of the measurement range. Proof-of-concept experiments demonstrate 1.66-kHz measurement rate with 1-m resolution over a 160 m sensing fiber length. Moreover, a measurement range of 2560 με with a precision of 20 με is successfully proved.

OCIS codes: (290.5900) Scattering, stimulated Brillouin; (060.2370) Fiber optics sensors; (040.2840) Heterodyne; (999.999) Brillouin distributed sensors; (999.999) Brillouin optical time domain analysis.

References and links

1. X. Bao and L. Chen, "Recent progress in Brillouin scattering based fiber sensors," Sensors (Basel) **11**(4), 4152–4187 (2011).
2. K. Y. Song and K. Hotate, "Distributed fiber strain sensor at 1 kHz sampling rate based on Brillouin optical correlation domain analysis," IEEE Photon. Technol. Lett. **19**(23), 1928–1930 (2007).
3. K. Y. Song, M. Kishi, Z. He, and K. Hotate, "High-repetition-rate distributed Brillouin sensor based on optical correlation-domain analysis with differential frequency modulation," Opt. Lett. **36**(11), 2062–2064 (2011).
4. R. Bernini, A. Minardo, and L. Zeni, "Dynamic strain measurement in optical fibers by stimulated Brillouin scattering," Opt. Lett. **34**(17), 2613–2615 (2009).
5. Q. Cui, S. Pamukcu, W. Xiao, and M. Pervizpour, "Truly distributed fiber vibration sensor using pulse base BOTDA with wide dynamic range," IEEE Photon. Technol. Lett. **23**(24), 1887–1889 (2011).
6. Y. Peled, A. Motil, and M. Tur, "Fast Brillouin optical time domain analysis for dynamic sensing," Opt. Express **20**(8), 8584–8591 (2012).
7. A. Zornoza, M. Sagues, and A. Loayssa, "Self-heterodyne detection for SNR Improvement and Distributed phase shift measurements in BOTDA," J. Lightwave Technol. **30**(8), 1066–1072 (2012).
8. M. González Herráez, K. Y. Song, and L. Thévenaz, "Arbitrary-bandwidth Brillouin slow light in optical fibers," Opt. Express **14**(4), 1395–1400 (2006).
9. A. Minardo, R. Bernini, and L. Zeni, "Stimulated Brillouin scattering modeling for high-resolution, time-domain distributed sensing," Opt. Express **15**(16), 10397–10407 (2007).
10. J. Humlícek, E. Schmidt, L. Bocánek, R. Svehla, and K. Ploog, "Exciton line shapes of GaAs/AlAs multiple quantum wells," Phys. Rev. B Condens. Matter **48**(8), 5241–5248 (1993).
11. A. Zornoza, D. Olier, M. Sagues, and A. Loayssa, "Brillouin distributed sensor using RF shaping of pump pulses," Meas. Sci. Technol. **21**(9), 094021 (2010).

Introduction

The increasing interest in structural health monitoring during the last few years has promoted the research and development of sensors capable to perform dynamic strain measurements [1–3]. In this context, Brillouin optical time domain analysis (BOTDA) sensors can provide distributed measurements of the strain profile in km-long fibers with high precision and spatial resolution. Nevertheless, a serious drawback of this technique is the requirement to scan the Brillouin gain spectrum (BGS) by sweeping the probe and pump frequency difference in order to obtain the Brillouin frequency shift (BFS) and hence the strain

#175723 - $15.00 USD Received 5 Sep 2012; revised 31 Oct 2012; accepted 7 Nov 2012; published 14 Nov 2012

distribution along the sensing fiber. This is a time-consuming procedure that restricts the use of the BOTDA technique to static measurements.

Recently, adaptations of the classical BOTDA scheme have been proposed for dynamic measurements. They are based on tuning the probe wave to the skirt of the BGS so that variations in BFS are translated to changes in the amplitude of the detected probe wave [4–6]. However, key challenges faced by these dynamic BOTDA sensors are to make measurements tolerant to variations in detected probe wave amplitude that are unrelated to strain changes, such as changes in the attenuation in the sensing fiber or in the pump power; also the improvement of the detected signal to noise ratio (SNR), so as to reduce the required averaging; and the increase of the measurement range.

In this paper, we propose and demonstrate a novel dynamic BOTDA sensor that is based on the use of the Brillouin phase-shift in addition to the conventional Brillouin gain. A phase-modulated probe wave is detected after Brillouin interaction with the pump and demodulated in the electrical domain. The RF phase-shift of the resultant signal is found to be dependent on the BFS, but independent of the Brillouin peak gain experienced by the probe wave and of the optical power detected. Therefore, BFS measurements based on this RF phase-shift are immune to attenuation variations in the fiber or changes in the power level of the pump pulses. Furthermore, the optical detection deployed can lead to an enhanced precision, to the broadening of the measurement range and to the enhancement of the measurement time.

Fundamentals

Figure 1 schematically depicts the fundamentals of the proposed system.

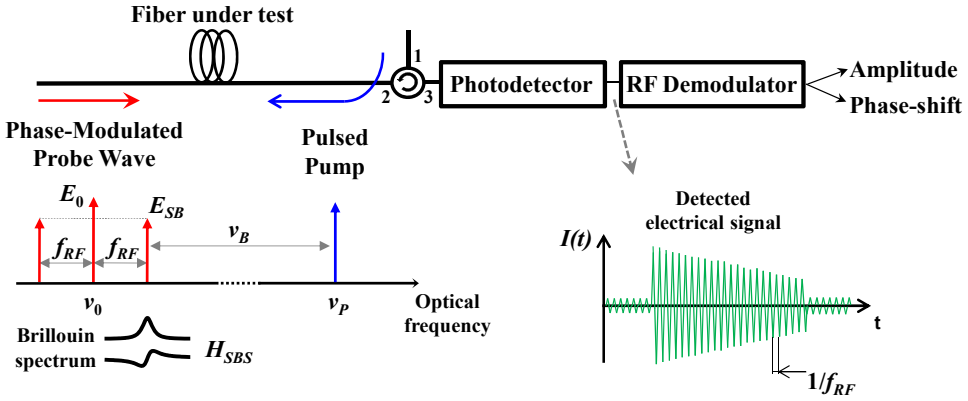

Fig. 1. Schematic representation of SBS interaction and the received signal.

A single tone phase-modulated probe wave is injected in one end of the optical fiber under test, while a pump pulse is introduced at the other end. This probe wave interacts with the pump pulse along the fiber via stimulated Brillouin scattering (SBS) and is directed to the receiver using a circulator. Finally, the detected electrical signal is demodulated in a synchronous demodulator [7]. If the modulation frequency is much higher than the Brillouin bandwidth, we can consider that SBS interaction only affects the upper sideband of the modulation. Then, the optical field at the input of the photodetector coming from the interaction of pump and probe at a particular location in the fiber, z, is given by the following expression:

$$E(t) = -E_{SB}\exp(j2\pi(\nu_0 - f_{RF})t) + E_0\exp(j2\pi\nu_0 t) + E_{SB}\exp(j2\pi(\nu_0 + f_{RF})t)H_{SBS}(\nu_0 + f_{RF}, z) \quad (1)$$

where E_0 and E_{SB} are the amplitudes of the optical fields of the carrier and first sidebands of the phase-modulated probe wave (higher-order sidebands were neglected, assuming a small

#175723 - $15.00 USD Received 5 Sep 2012; revised 31 Oct 2012; accepted 7 Nov 2012; published 14 Nov 2012

modulation index), ν_0 is the optical frequency of the carrier, f_{RF} is the modulation frequency and H_{SBS} is the complex Brillouin gain spectrum at position z, which can be described by:

$$H_{SBS}(\nu,z) = \exp(G_{SBS} + j\varphi_{SBS}) \approx (1+G_{SBS})\exp(j\varphi_{SBS}) \tag{2}$$

where G_{SBS} and φ_{SBS} are the Brillouin gain and phase-shift, respectively. The approximation in the second term is obtained assuming a small gain, which is the case for BOTDA sensors. In the case of employing pump pulses longer that the acoustic lifetime, the spectrum is Lorentzian:

$$H_{SBS}(\nu,z) = \left(1+\frac{g_B \Delta\nu_B{}^2}{\Delta\nu_B{}^2 + 4\Delta\nu^2}\right)\exp\left(-j\,\frac{2g_B\Delta\nu\Delta\nu_B}{\Delta\nu_B{}^2+4\Delta\nu^2}\right) \tag{3}$$

where g_B is the peak gain, $\Delta\nu_B$ is the Brillouin linewidth, $\Delta\nu = \nu - \nu_P + \nu_B(z)$ is the detuning of the interaction frequency from the center of the Brillouin spectrum, ν_P is the optical frequency of the pump wave and ν_B is the Brillouin frequency shift at position z. For pump pulses shorter than the acoustic lifetime, the effective interaction spectrum is broadened and cannot further be considered Lorentzian. In this case, the interaction spectrum is derived taking into account the pulse bandwidth [8, 9].

The detected optical power signal at f_{RF} can be expressed as:

$$\begin{aligned} P(t)\big|_{f_{RF}} &= E_0 E_{SB}\left[(1+G_{SBS})\cos(2\pi f_{RF}t + \varphi_{SBS}) - \cos(2\pi f_{RF}t)\right] \\ &\approx \frac{4E_0E_{SB}g_B\Delta\nu_B}{\sqrt{\Delta\nu_B{}^2+(2\Delta\nu)^2}}\cos\left(2\pi f_{RF}t - \arctan\left(2\frac{\Delta\nu}{\Delta\nu_B}\right)\right) \end{aligned} \tag{4}$$

where the last term has been obtained assuming small g_B. Notice, that in Eq. (4) the detected RF phase-shift is independent of the particular Brillouin gain peak experienced by the probe wave and of the received optical power. This is highlighted in Fig. 2, where the RF phase-shift in our system and the amplitude in a conventional gain-based BOTDA are calculated and represented for different values of g_B. As it is shown, the RF phase-shift traces are identical for the different values of g_B. This fact has major implications for dynamic sensing. The strain measurements of conventional dynamic BOTDA are based in setting the probe wave to a wavelength on the slope of the amplitude spectrum and translating changes in the detected probe amplitude to variations in BFS. The amplitude spectrum is sensitive to variations in pump power or attenuation in the fiber. Therefore, these measurements are susceptible to errors, which are highly probable in a structure with dynamic deformation, where they would be misinterpreted as strain changes. In the method proposed in this paper, these errors are avoided by employing the phase-shift spectrum of the detected RF signal, instead of the amplitude spectrum. As it is schematically depicted in Fig. 2(b), the probe wave is set to the slope of the detected phase-shift, obtaining a measurement that is immune to variations of the pump power (via g_B) and of the received probe power.

#175723 - $15.00 USD Received 5 Sep 2012; revised 31 Oct 2012; accepted 7 Nov 2012; published 14 Nov 2012

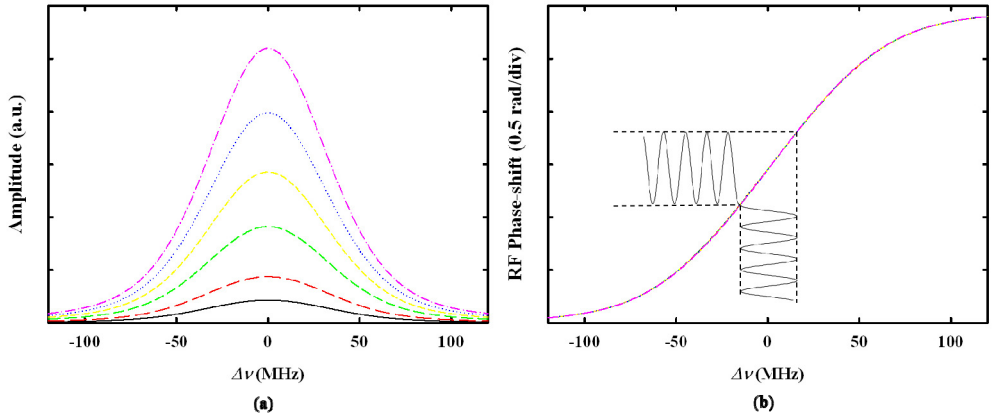

Fig. 2. Calculated (a) amplitude at conventional BOTDA and (b) RF phase-shift of the proposed technique for different values of g_B. In (b) the effect of a variation in BFS on the detected RF phase-shift is schematically depicted (black sinusoids) to highlight the dynamic measurement principle.

The phasor diagram in Fig. 3 further clarifies the reason for this independence of the detected RF phase-shift, θ_{RF}. It depicts the interference of the two beat terms in Eq. (4) that result from the detection of the phase-modulated probe. The real and imaginary parts of the phasor affected by Brillouin interaction can be obtained by multiplying its amplitude by $\cos(\varphi_{SBS})$ and $\sin(\varphi_{SBS})$ respectively. If small Brillouin gain is assumed, these two terms can be approximated to 1 and φ_{SBS} respectively, as shown in the figure. Therefore, the real and imaginary parts of the phasor representing the resultant RF signal are proportional to the Brillouin gain and phase-shift, respectively, which in turn are both directly proportional to the Brillouin peak gain as it is shown in Eq. (3). Therefore, any change in g_B will just change the detected RF amplitude, but not its phase-shift. This is found to be valid for Lorentzian interaction as well as for other Brillouin spectra resulting from the use of narrow pump pulses.

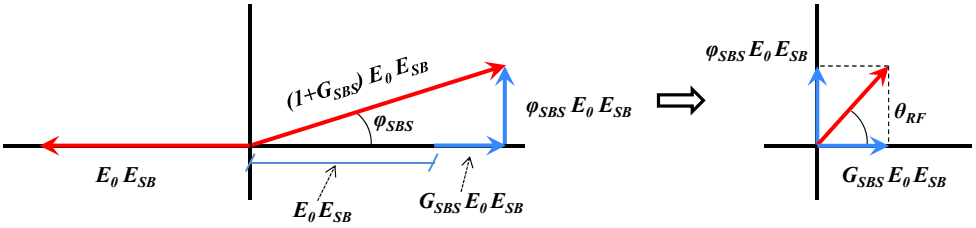

Fig. 3. Phasor diagram of the detected RF signal.

Another important issue to consider in dynamic sensing is the precision of the measurement. According to the measurement principle explained above, this can be calculated taking into account the received noise and the slope of the function used to translate BFS variations into amplitude (in conventional BOTDA) or phase-shift changes (in our scheme). Figure 4 compares the precision of our technique to that of the conventional BOTDA. This has been calculated by considering Gaussian noise in the received signals of both systems and assuming Gaussian pulses of short duration, whose effective interaction spectrum can be approximated to a Faddeeva function [10]. In addition, just one of the two possible sides of the amplitude spectrum for conventional BOTDA is depicted.

#175723 - $15.00 USD Received 5 Sep 2012; revised 31 Oct 2012; accepted 7 Nov 2012; published 14 Nov 2012

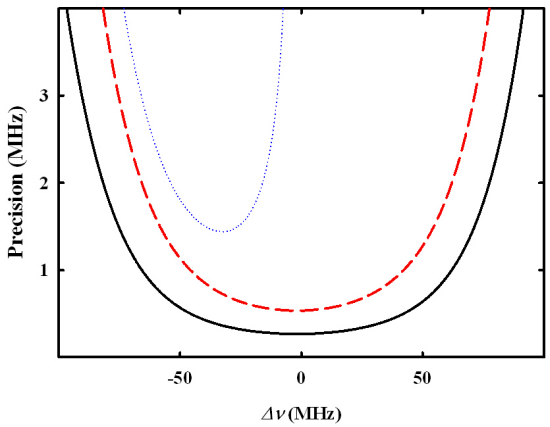

Fig. 4. Calculated BFS precision for the conventional BOTDA (dotted line) and phase-shift technique (dashed line), both with an equal SNR of 44dB, and for the phase-shift technique with 6-dB SNR enhancement (solid line).

As it is shown in the figure, the phase-shift technique obtains greater measurement range for a given precision than that of the conventional BOTDA. For instance, for a precision of at least 1 MHz (around 20 με for standard single mode fiber) the measurement range would be 88 MHz (1760με) for the phase-shift technique, while the conventional BOTDA cannot even reach this precision for the same conditions. Furthermore, note that Eq. (4) shows that the detected signal and its SNR can be enhanced simply by increasing the carrier power, while keeping the sidebands power low enough to avoid non-local effects [7]. For example, if this feature is exploited to achieve a 6-dB SNR improvement, this would result in an enhanced measurement range of 127 MHz (2540 με) with 1 MHz precision, as it is highlighted in Fig. 4.

Furthermore, according to the measurement principle followed in dynamic BOTDA sensors, there is a direct dependence of the measurement range on the spectral shape employed to translate variations of BFS into amplitude or phase-shift changes. Therefore, the use of shorter pump pulses broadens the interaction spectrum and hence increases the measurement range. Figure 5 illustrates this procedure by comparing the RF phase-shift spectrum and BFS measurement precision for two pump pulses of different temporal duration. As it is shown, the measurement range of the sensor is enlarged from 74 MHz (1480 με) to 88 MHz (1760 με) for a 1 MHz (20 με) target precision. However, this assumes constant SNR, which in practice requires additional averaging.

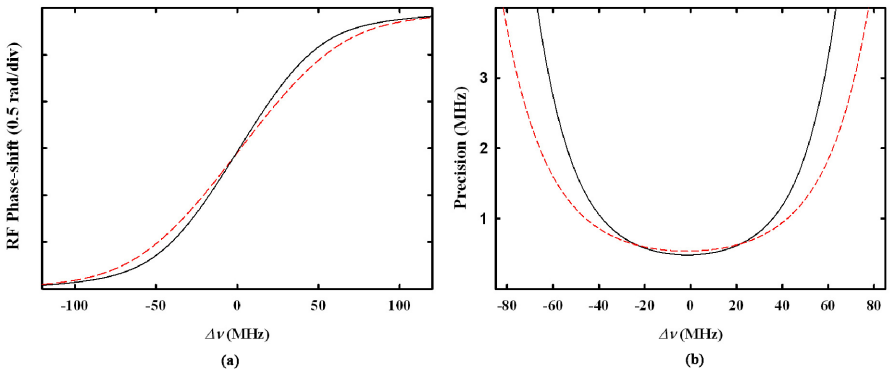

Fig. 5. Calculated (a) RF phase shift of the proposed technique for two Gaussian pulses of 40 MHz (red dashed line) and 30 MHz (black solid line) bandwidth and (b) precision of both pulses for a SNR equal to 44dB.

#175723 - $15.00 USD Received 5 Sep 2012; revised 31 Oct 2012; accepted 7 Nov 2012; published 14 Nov 2012

Experimental Setup and measurements

The experimental setup shown in Fig. 6 was assembled in order to demonstrate the system. The output of a 1559.7-nm laser source is divided in two optical branches with an optical coupler. In the upper branch, the optical pump pulses are formed using a Mach-Zehnder electrooptic modulator (MZ-EOM) by the RF pulse-shaping technique so as to obtain clean and leakage-free pulses [11]. After amplification in an erbium doped fiber amplifier (EDFA), the resulting pump pulses are directed via a circulator to a 160m-long fiber. In the lower branch, the probe wave is generated with an electro-optic phase modulator driven by a 850 MHz RF signal. After interacting with the pump pulses via SBS, the probe signal is directed to a receiver and the resultant RF signal is demodulated [7]. Finally, the BOTDA signal is captured in a digital oscilloscope.

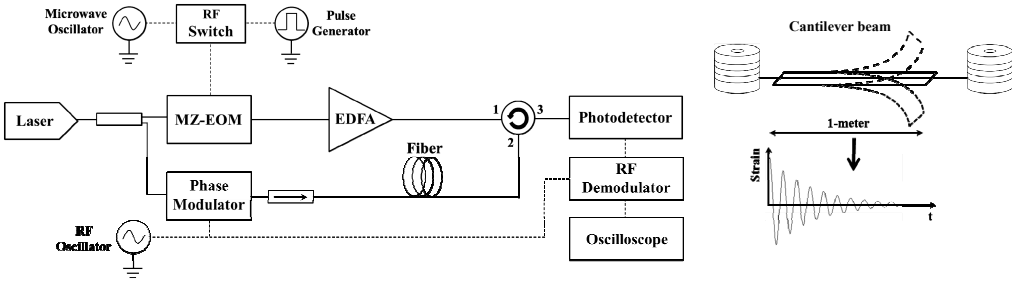

Fig. 6. Experimental setup for the phase-shift-based BOTDA dynamic strain measurements.

In order to prove that the detected phase-shift is immune to amplitude changes of the BOTDA signal, several spectra were measured varying the attenuation of the probe and pulse signals. The pulse duration was set to 10 ns corresponding to 1 m spatial resolution. Figure 7 shows that, indeed, the detected RF phase-shift remains unaltered while the amplitude suffers severe attenuation.

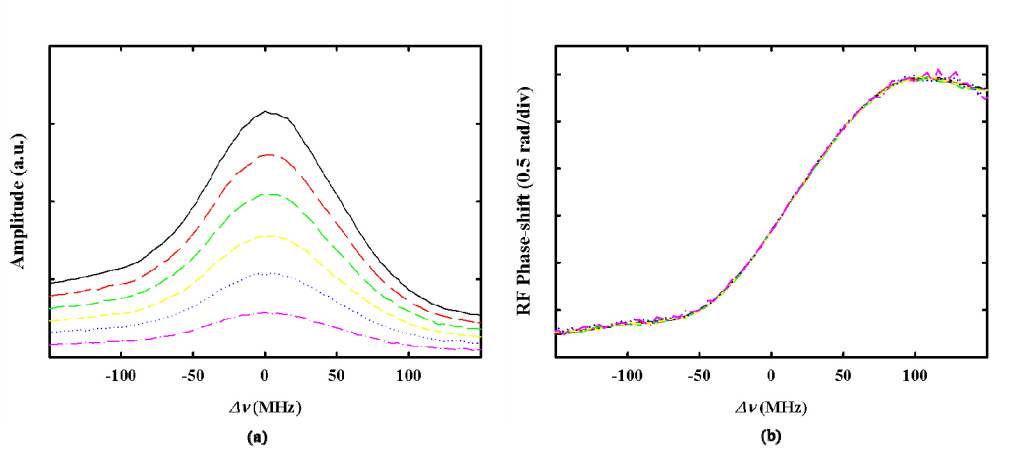

Fig. 7. (a) Amplitude and (b) phase-shift spectra for different attenuation values of the pulse and probe signals.

In addition to this, the measurement range achieved by the phase-shift technique was measured for two different pulse durations of 9 ns and 10 ns. This is represented in Fig. 8(a). The measurement range achieved for a precision of 1 MHz is 76 MHz (1520 με) for the 10 ns pulse in contrast to 84 MHz (1680 με) for the 9 ns pulse. These results were derived from the measurement of 25 RF phase-shift spectra using 64 averages at the oscilloscope capture. As it is shown, the effective interaction spectrum is broadened by employing shorter pulses and a greater measurement range is obtained. Furthermore, the precision achieved for a given pulse

#175723 - $15.00 USD Received 5 Sep 2012; revised 31 Oct 2012; accepted 7 Nov 2012; published 14 Nov 2012

duration can be enhanced by increasing the SNR of the detected signal, simply by increasing the averaging at the oscilloscope. For instance, for a 9 ns pulse and a minimum precision of 1 MHz, the measurement range is 128 MHz (2560 με) when using 128 averages.

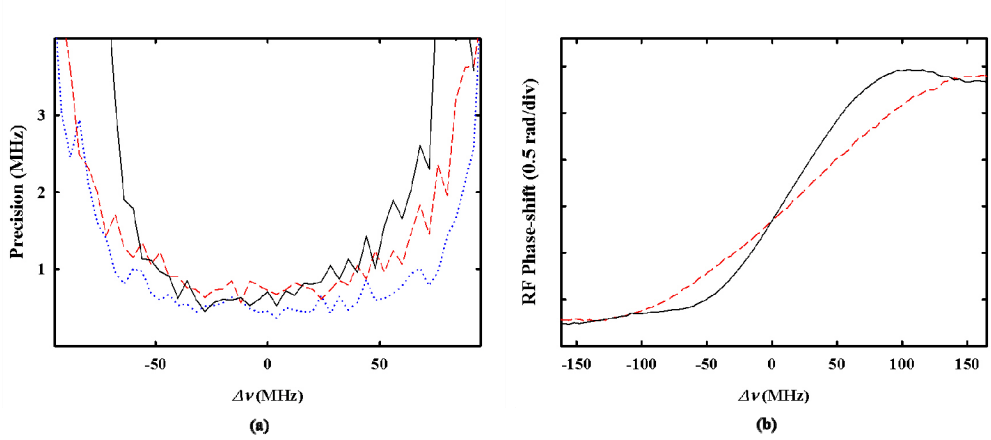

Fig. 8. (a) BFS Precision achieved for the phase-shift technique using pulses of 9 ns with 64 averages (red dashed line) and 128 averages (blue dotted line), and for pulses of 10 ns with 64 averages (black solid line). (b) RF phase-shift spectra for pulses of 9 ns (red dashed line) and 10 ns (black solid line).

Finally, the last 1-meter section of the 160-m fiber was affixed by epoxy resin onto the surface of a 1-m cantilever beam. The cantilever beam was made to vibrate so that dynamic distributed measurements of the induced strain along the fiber could be performed. The pulse duration was set to 10 ns, with a measurement rate of 1.66 kHz, achieving a precision of 20 με with a moving window averaging of 64 samples. Notice that this sampling rate was limited by the available acquisition instrumentation, so that higher measurement rates maintaining the same precision should be possible. Figure 9 shows the measured strain in the fiber at the cantilever beam location when this is made to vibrate. Notice that the measured strain corresponds to the averaged strain on the 1-m beam, as the strain amplitude is not uniform along the cantilever beam and the resolution of the distributed measurement is 1 m.

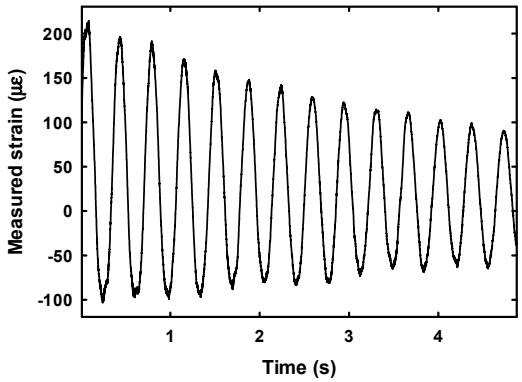

Fig. 9. Fast-acquisition phase-shift-based measurement of the induced strain at the cantilever beam.

#175723 - $15.00 USD Received 5 Sep 2012; revised 31 Oct 2012; accepted 7 Nov 2012; published 14 Nov 2012

Conclusions

A novel dynamic Brillouin sensor based on the use of the Brillouin phase-shift has been proposed and demonstrated. The technique relies on the RF phase-shift spectrum, which is shown to be largely immune to variations of the Brillouin peak gain, attenuation on the fiber, or changes in the power of the pump pulses. Therefore, one of the fundamental drawbacks of the previously reported dynamic BOTDA schemes is overcome. In addition, this technique enables a broadening of the measurement range by simply improving the SNR or reducing the pulse duration. In this way, larger measurement ranges, with enhanced spatial resolution can be achieved. Furthermore, a fast dynamic strain measurement was performed in a cantilever beam with high measurement range and precision.

Acknowledgments

The authors wish to acknowledge the financial support from the Spanish Ministerio de Educación y Ciencia through the project TEC2010-20224-C02-01 and from the Universidad Pública de Navarra.

#175723 - $15.00 USD Received 5 Sep 2012; revised 31 Oct 2012; accepted 7 Nov 2012; published 14 Nov 2012